

# SnapHand: A Dexterous Low-Cost Tendon-Driven Biomimetic Robotic Hand with Novel Snap-fit Pin Joints

Changan Chen, Yuan Jiang, Ethan Marot, Nicolas Pfitzer, Alexandre Clin Deffarges

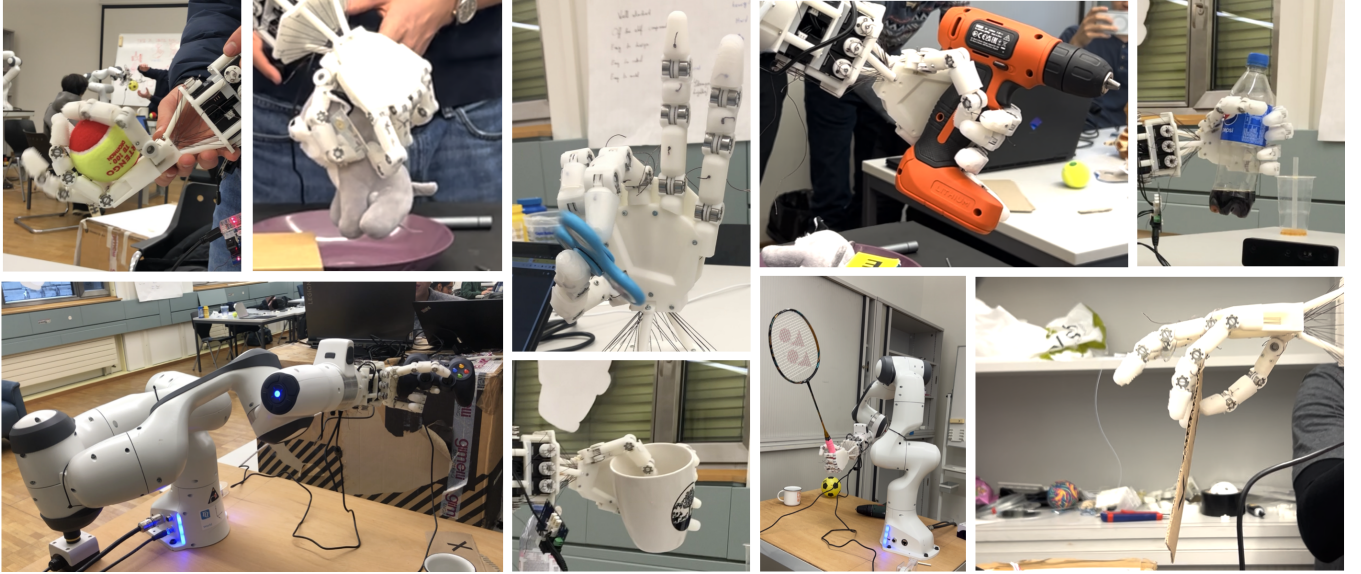


Fig. 1: **Snap Hand performing various manipulation and grasping tasks.** The Snap Hand is a low cost tendon driven robotic hand with novel snap-fit pint joints. Its highly biomimetic form enables a wide range of general manipulation tasks such as rolling a tennis ball in-hand, spinning a fidget spinner, grasping and holding various objects in a human-like manner.

**Abstract**—The field of embodied AI and robotics has seen rapid advancements, with increasing demands for dexterous robotic hands capable of performing versatile real-world tasks. However, existing biomimetic dexterous robotic hands are often hindered by high costs and maintenance complexities, limiting their accessibility and practical application. In response to these challenges, this paper introduces the SnapHand: a cost-effective, tendon-driven dexterous biomimetic robotic hand. The SnapHand features a novel snap-fit pin joint design, enabling rapid assembly and maintenance. Despite its affordability and simplicity, the SnapHand does not compromise on functionality, with 11 actuated degrees of freedom (DoF) and the ability to perform various dexterous tasks at a cost of only \$900. Our extensive teleoperation experiments, leveraging an optimization-based hand-tracking and re-targeting algorithm, demonstrate the hand’s high level of dexterity and capability. Additionally, we show the SnapHand’s proficiency in executing dexterous reinforcement learning tasks. This study showcases how advanced robotic hand capabilities can be achieved within the constraints of affordability and simplicity, paving the way for broader accessibility and application in the field.

## I. INTRODUCTION

In recent decades, robotic systems have revolutionized industries from manufacturing and healthcare to space exploration. With the rapid advancement of embodied AI and robotics, the era of personal robotic assistance is approaching a transformative phase. The integration of robots into our daily lives comes the pressing need for robotic systems

that seamlessly interact with humans and their surroundings. One of the pivotal components in achieving this vision is a versatile gripper capable of interacting with a wide range of shapes and tools. These hands should be capable of performing real-world tasks, be cost-effective, and easy to maintain. Currently, the most commonly used robotic hand in the industry is the simple two-finger gripper, which has only one degree of freedom. Recent research indicates that robots equipped with such grippers can perform a variety of tasks [1]. However, a biomimetic anthropomorphic design offers significantly greater dexterity, which could enable the execution of complex tasks such as rolling a ball [2], solving a Rubik’s cube [3], or handling electronic components with tweezers [4]—activities that are challenging or time-consuming for simpler grippers. Furthermore, an anthropomorphic design facilitates learning from human demonstration videos [5], [6], [7], which are abundantly available.

Unfortunately, current biomimetic dexterous robotic hands often face limitations due to their high cost and maintenance challenges, restricting their widespread market adoption and accessibility for research groups. For instance, the Shadow Hand [8] developed by Shadow Robotics and used by OpenAI for tasks like solving a Rubik’s cube, utilizes a tendon-driven mechanism and features 22 active degrees of

freedom (DoF), is priced at over 100,000 USD. Another example, the Allegro Hand [9], is a direct motor-driven robotic hand with four fingers. Priced at 16,000 USD, it is frequently criticized for its unreliability and maintenance difficulties. Additionally, ILDA [4], a novel hand based on a spatial linkage-driven mechanism, although compact and robust, presents challenges in assembly and maintenance due to its numerous linkage components.

To enhance the accessibility of dexterous robotic hand hardware, it is essential to ensure affordability, ease of assembly, maintenance, and repair, utilizing minimal assembly techniques and basic equipment like hobby-level 3D printers and inexpensive fasteners. Additionally, the hand should possess multiple degrees of freedom (DoF), ideally at least 2 DoF for each finger and in total more than 10 DoF for the hand, to ensure adequate capability. In this context, we introduce the SnapHand, a cost-effective and dexterous tendon-driven biomimetic robotic hand featuring innovative *snap-fit* pin joints. This hand is comprised of finger and palm components that can be rapidly printed using a hobby-level 3D printer, specifically the Prusa MK3S. It incorporates fishing line tendons and readily available fasteners and bearings. The SnapHand has 11 actuated DoFs and 16 novel pin joints, enabling it to perform a variety of dexterous tasks, all at a cost of just 900 USD.

The SnapHand employs a tendon-driven design as its driving mechanism, positioning the actuators away from the joints and using tendons to transmit force for joint actuation. This approach results in a slimmer finger design with low inertia, thereby minimizing control efforts. In contrast to the LEAP hand [10], which utilizes a direct drive design, our tendon-based SnapHand offers increased compliance at the joints and reduces the risk of motor exposure to direct impacts. Furthermore, unlike the Faive Hand [2], a low-cost robotic hand with a rolling contact joints design, we have developed a novel type of pin joint incorporating bearings. This innovation significantly simplifies finger kinematics and state estimation, reducing them to the absolute minimum. Additionally, it greatly simplifies assembly, allowing a finger to be assembled in mere minutes without specialized techniques, experience, or fixtures needed, marking a substantial improvement over conventional pin joints.

Despite its cost-effectiveness and ease of assembly, the proposed SnapHand exhibits remarkable dexterity and capability. We have conducted comprehensive teleoperation experiments using our specialized optimization-based hand-tracking and re-targeting algorithm, as highlighted in fig. 1 and further detailed in the experiments section. Moreover, the SnapHand's ability to perform dexterous reinforcement learning (RL) tasks, such as rolling a ball — trained using IsaacGym [11] — in an open-loop fashion on our hardware, is a testament to its practical functionality. This demonstrates that high dexterity and advanced capabilities of SnapHand, even when adhering to constraints of affordability and simplicity in assembly.

In this work, we propose the following contributions

- Present a novel pin-joint design that allows fast finger

assembly in mere minutes, reducing assembly time by a factor of 10;

- Introduce the prototype version of the *SnapHand*, designed as easily maintainable and accessible dexterous manipulation hardware platform.
- Leverage vision-based hand and wrist tracking for intuitive teleoperation;
- Apply an open-loop policy trained in simulation on a ball rolling task.

## II. RELATED WORK

**Actuation Mechanism** There are three primary types of actuation mechanisms employed in robotic hands. (1) *Direct drive* robotic hands feature motors typically located in the phalanges, with the joint's rotational axis either directly coupled to the motor shaft or connected through gears or timing belts. [12], [13] This actuation offers high joint efficiency and straightforward joint arrangement without the need for additional transmission components. However, the use of sizeable actuators often results in bulkier fingers and increased phalangeal inertia. Furthermore, the motors' direct exposure to manipulated objects increases susceptibility to damage from unanticipated impacts. (2) *Linkage-driven* robotic hands incorporate complex planar or spatial linkage systems [4] for each finger, controlled by linear actuators housed within the palm or forearm. These designs provide effective bidirectional joint control and can leverage parallel linkage mechanisms to enhance structural rigidity and grasping force. Nonetheless, they typically face challenges in maintaining a large workspace, as the structural integrity requires a dense arrangement of robust linkages within a limited space. High-precision assembly and maintenance also present significant challenges for this design. (3) *Tendon-driven* robotic hands [2], [14], [15] are actuated by tendons, with one end anchored to the phalanges and the other wound around a spool on a rotational actuator's shaft. This design is the most biomimetic among the three, often easier to manufacture with materials such as 3D-printed parts and standard fasteners. The tendon-driven system also positions the actuators remotely from the hand, minimizing actuator damage risk from external impacts and reducing the inertia of the fingers and hand.

**Joint Types** Robotic hands employ four predominant joint types, each with different variations. (1) *Synovial joint* mimics the human finger joint but presents significant challenges in construction. Recent advancements in [16] have demonstrated that advanced vision-controlled 3D inkjet printers can fabricate the entire structure in a single print; however, this technology remains largely inaccessible and potentially costly. Additionally, the complex behavior of synovial joints complicates accurate modeling, state estimation, and control. (2) *Flexure joint* uses a flexible material to connect phalanges [17], offering the benefit of low friction and straightforward manufacturing. Yet, its representation in simulations can be challenging, and the elastic material is susceptible to wear with frequent use. (3) *Rolling contact joint* employs ligaments to join phalangeal parts, permitting rolling motion

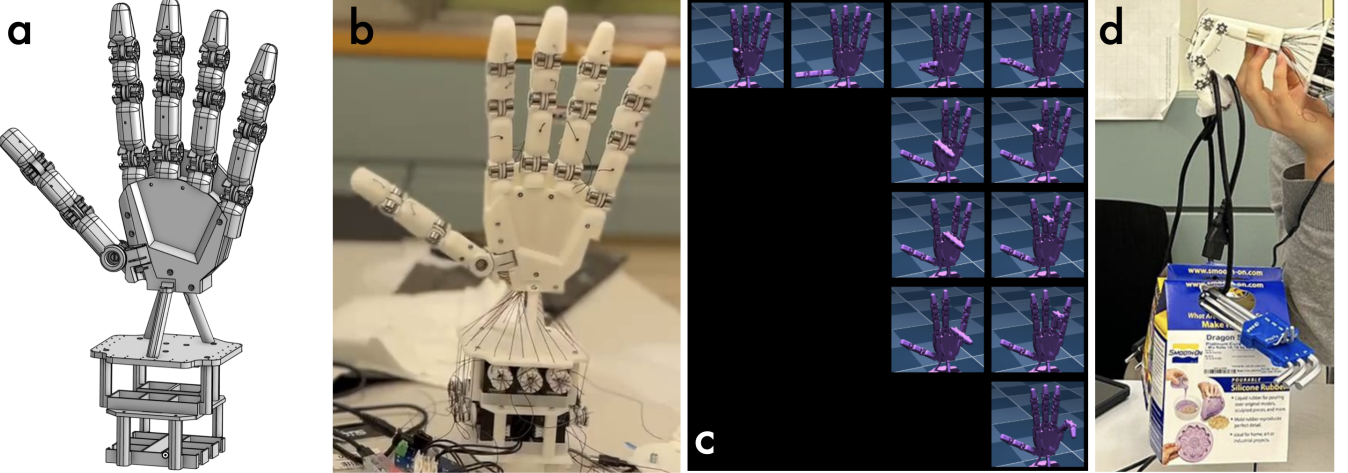


Fig. 2: **The Snap Hand is by design bio-mimetic both in its shape and degrees of freedoms (DoFs).** a) The CAD model of the Snap Hand. b) The 3d printed prototype with bearings and motors mounted. c) The 11 DoFs over the five fingers. Each row represents a finger (thumb, index finger, middle finger, ring finger, little finger from top to bottom). d) Snap Hand lifting up a payload of 2.2kg with downward facing palm.

at the contact surface. The introduction of fluid [18] for joint lubrication and improved impact absorption has been documented; despite its manufacturing simplicity and low friction, the joint’s performance heavily depends on the precise installation of ligaments, complicating finger kinematics and joint state estimation. (4) *Pin joint*, a traditional design, uses a mechanical pin as the rotational axis between two phalanges, offering simple kinematics and ease of state estimation—attributes favorable for low-cost robotic hands. Our enhancements to the traditional pin joint design have addressed its rigidity and manufacturing challenges, refining its suitability for cost-effective robotic applications.

**Teleoperation** Robotic hand teleoperation is mainly categorized into three classes: gloves assisted, marker based and bare hand. In [19] and [20], color markers are used to track the keypoints of the human hand, whereas there are also commercially available gloves such as CyberGlove [21], HaptX [22] and Manus Meta VR glove [23] that provide accurate hand tracking. Despite their high tracking accuracy, bare hand tracking is more desirable due to its low cost and minimal hardware requirements. Thanks to the advancements in deep learning, various methods are proposed to give reliable human hand tracking [24] [25] [26]. We use the hand tracking solution from Mediapipe [26] which is light weight and only requires a single RGB-D camera. To achieve the teleoperation, the tracked human hand needs to be retargeted to the robot hand. Many works adopted a keyvector optimization based method [25] [7]. Although it is general to all kinds of morphology of robotic hands, the multiple losses and parameters involved makes it hard to tune and prone to local minima. Since Snap Hand is highly biomimetic, a direct angle mapping [10] can achieve reasonable teleoperation. Therefor we use an affine transformation of the angles calculated from the tracked human hand as initialization, and engage an optimization step to optimize the pinch if

necessary.

**Reinforcement Learning** Robotic hands have been coupled with reinforcement learning techniques to be able to learn complex manipulation tasks [2] [3] [4]. It is therefore essential for a viable robotic hand to be able to be adequately simulated in a virtual environment in order to be able to deploy trained reinforcement learning policies. From a kinematics model created in the MuJoCo software, said model was then imported into NVIDIA’s Isaac Gym. Combined with the “rl\_games” library, we used the pre-existing “faive\_hand” reinforcement learning repository to train our hand and export our policy, while modifying both the cost function as well as the simulation environment and parameters, to produce a virtual Snap Hand whose behavior can be rolled out accurately onto its real world counterpart.

### III. DESIGN

In this section, we introduce the design of the Snap Hand including the basic considerations in terms of the joint actuation and distribution of the degrees of freedoms (DoFs) (section III-A), an essential novel pin joint design we propose to simplify the assembly process and to enable the dislocation feature of human joints (section III-B), and finally the modelling and control of the hand (section III-C).

#### A. Hardware Overview

The Snap Hand has 16 pin joints distributed over 5 fingers, as shown in fig. 2 a and b. The thumb has 4 independently actuated joints, including two joints for simulating the carpometacarpal (CMC) joint, one metacarpophalangeal (MCP) joint and one distal interphalangeal (DIP) joint. Each of the other four fingers consists of three joints, MCP, proximal interphalangeal (PIP) joint and DIP. The PIP and DIP are coupled through interior tendons, while the MCPs are actuated with dedicated motors, except for the little finger, where all three joints are coupled. The distribution of the DoFs are

due to the consideration of using as few motors as possible and that the thumb is essential for accomplishing many dexterous tasks while the little finger is mainly for providing support. The actuated DoFs are illustrated in fig. 2 c.

The human-like finger and palm design together with the carefully distributed DoFs results in the biomimetic form of the Snap Hand. With only a self weight of 0.67kg, it can lift up a payload of 2.2kg with palm facing downwards as shown in fig. 2 d.

### B. Snap-Fit Pin Joint

We opted for the pin joint design due to its benefits of simple kinematics and ease of state estimation, as detailed in section III-C. Commonly, pin joint designs [8], [27], [28], [29] involve manufacturing the phalanges as a single piece, using a mechanical pin as the rotational axis. This approach ensures the alignment of pin holes on opposite sides of the phalanges. However, it can lead to high friction under heavy loads due to the direct contact between the pin and phalanges. Additionally, the typically small diameter of the pins makes them susceptible to damage from impacts. To address these issues, some designs [30] incorporate bearings as the rotational axis. Yet, this introduces its own challenges: either a thin pin with fasteners is required, or the phalanges must be split longitudinally to install the second phalange. This increases manufacturing complexity, as precise alignment and accuracy become critical factors.

Traditional pin joints are frequently criticized for their high friction, manufacturing complexity, and susceptibility to structural damage under overstress, which can be challenging to repair. Additionally, these joints often lack compliance due to their inherent stiffness. Consequently, many researchers have explored alternative joint designs, such as rolling contact joints [2], [18], ellipsoid contact joints [31], or flexure

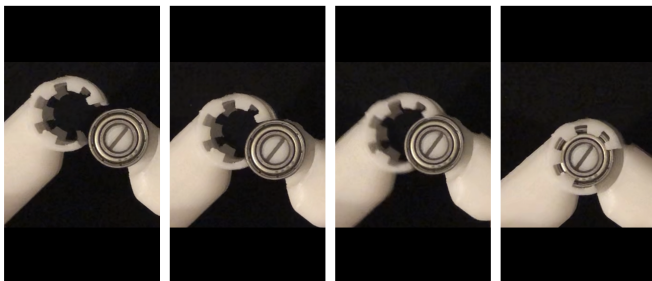


**Fig. 3: Snap-fit Assembly Process.** The sequence demonstrates the straightforward snap-fit method employed in the assembly of our robotic hand’s joints. Initially, the bearing is aligned with the opening on the phalange (first image). As pressure is applied, the bearing is guided into place by the arc-shaped component of the phalange (second image). Once the bearing edges reach the retention features, the components are pressed together until they click into position (third image), resulting in a secure and aligned joint without the need for additional fasteners (fourth image). This intuitive snap-fit design ensures quick and effortless assembly, significantly reducing construction and maintenance time.

joints [17]. These alternatives offer greater compliance owing to their elastic structures and are more resilient to sudden impacts, tending to dislocate rather than break.

In SnapHand, as illustrated in fig. 3, we introduce a novel type of pin joint designed to address the limitations of traditional pin joints. This innovative joint comprises a major arc-shaped component on one phalange and a pair of parallel-installed bearings on the other. These components can be effortlessly assembled through a snap-fit process. Each phalange is 3D-printed as a single piece, ensuring alignment precision that is only limited by the printer’s maximum accuracy, eliminating the need for fixtures during assembly. The use of relatively large yet lightweight bearings in the joint allows for high load capacity with minimal friction and inertia, facilitating a smoother sim-to-real transition of reinforcement learning (RL) policies. The gear-like periphery of the arc not only limits lateral motion between the phalanges but also mitigates stress concentration during snap-fit installation, reducing the risk of cracking. Moreover, the elasticity of the receiving phalange part introduces a dislocation capability, previously unattainable in pin joints. This feature enhances the joint’s robustness and longevity while maintaining the simplest finger kinematics.

Our innovative pin joint design significantly simplifies the assembly process: each finger comprises only three 3D-printed parts, six bearings, and six tendons, and can be assembled in just a few minutes. We assert that this design is considerably easier to assemble and maintain than rolling contact joints. Typically, rolling contact joints require a specially designed fixture tool for installing and fastening the ligaments that connect the phalanges. This process is not only time-consuming but also demands specific assembly skills. Moreover, in cases where rolling contact joints fail due to sudden impact loads, the ligaments often break, necessitating a complete reinstallation. The quality of this reinstallation directly influences the functionality of the repaired hand and varies depending on the technician’s skill.

In contrast, our design allows for quick reattachment of dislocated phalanges in seconds, enabling immediate repair of the SnapHand. In extreme cases where a phalange breaks, replacement parts can be readily printed in under 30 minutes using a hobby-level 3D printer.

### C. Kinematics and Control

All joints are tendon-driven and controlled by in total 11 Dynamixel XC330-T288-T servo motors. Each actuated joints has two tendons routed antagonistically around it and through the center of rotation of the previous joints, such that the controlling of one joint is independent of the previous ones. With this routing, each actuated DoF can be controlled by one motor independently in both directions. This results in the following simple kinematic model.

$$q = \frac{R}{r}(p - \bar{p}), \quad (1)$$

where  $q$  is the joint angle,  $p$  the motor position,  $\bar{p}$  the neutral motor position,  $r$  and  $R$  the joint and the spool radius,

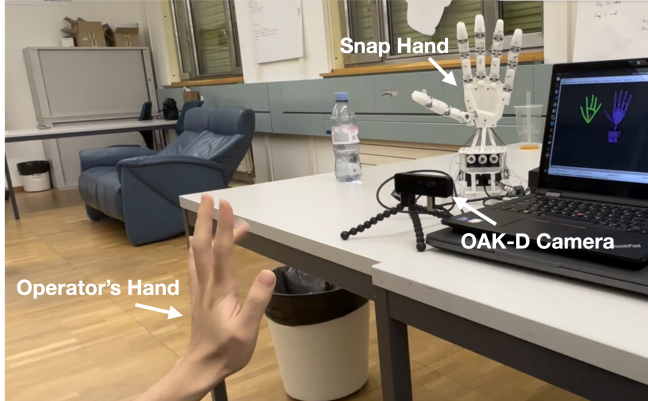


**Fig. 4: Vision based teleoperation setup.** An OAK-D camera is used to capture the human hand before the captured hand is tracked by the hand tracker from Mediapipe [26]. The tracked hand configuration is then remapped to the Snap Hand before the corresponding motor command is sent to motors.

respectively. With these simple kinematics, the desired joint angles are directly converted into desired motor positions and commanded to the Dynamixel motors. The state estimation is therefore also straightforward through the constant ratio between the current joint angles and the motor positions.

#### IV. VISION-BASED TELEOPERATION

We use a single OAK-D camera to capture the operator’s hand. The hand is tracked using the hand tracker from Mediapipe [26]. The setup is illustrated in fig. 4. The tracked human hand is then retargeted to the Snap Hand through a two stage algorithm. First the human hand joint angles are calculated from the keypoints output by the hand tracker and mapped to the Snap Hand joint angles through an affine transformation as initialization. If two of the operator’s finger tips are closed enough, the respective finger tips of the Snap Hand are enforced to be close to each other by minimizing the corresponding distance. This pinch optimization step is achieved through few gradient descent steps with the differentiable forward kinematics. Empirically, we find this better than the provided simplified version of keyvector optimization based retargeting algorithm [7] in the sense that it is easier to tune and avoids the problem of balancing multiple losses and being stuck at local minima.

#### V. REINFORCEMENT LEARNING

The Snap Hand’s kinematics model is imported into NVIDIA’s Isaac gym (see fig. 5), from there a reinforcement learning (RL) pipeline is created with the goal of rotating a ball in two possible directions at a desired minimum angular velocity. Due to the five digits of the hand, the agent initially wanted to minimize total torque per its cost function. This lead to only three digits rotating the ball, and the other two laying in their neutral extended positions. However, converting this strategy into the real world would lead to low robustness. Therefore additional noise is inserted into

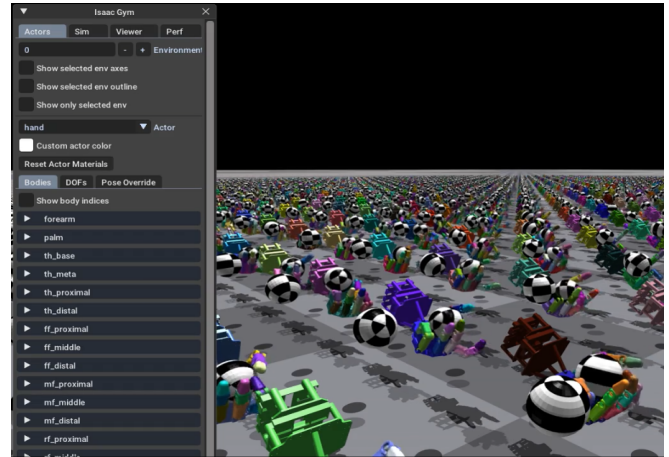


**Fig. 5: RL environment.** Thousands of agents are trained parallel to accelerate the learning process.

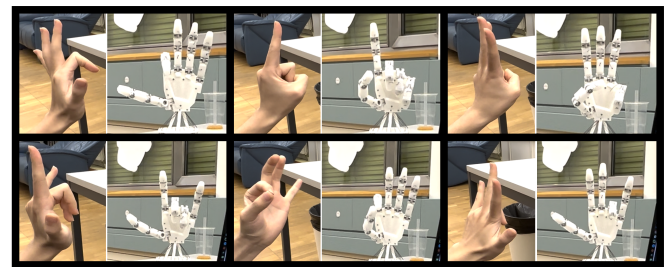


**Fig. 6: Accurate gesture copy.** Thanks to its biomimetic nature, the Snap Hand can follow the operator’s hand accurately, performing dexterous gestures such as pinch.

the simulation leading to perturbations in the ball’s position and velocity. This combined with an increased penalty for dropping the ball leads to the agent to using all five fingers in order to ensure the ball is in a stable configuration. When bridging the Sim2Real gap, an open loop simulation policy records joint angles and exports them to be recreated by the physical hand. Both the frequency at which the commands are received as well as the servo motors upper current threshold are decreased so that the policy is easier to observe and fine tune and to minimize the risk of hardware failure. In the physical world, the ball often slips between the contact surfaces, diminishing the achieved angular velocity. We think that this is due to difference between the simulated ball size and the ball the policy was tested on. Higher friction via the design of specific material padding on key finger points could also help ensure that the policy behaves optimally when tested in the real world.

## VI. EXPERIMENTS

### A. Dexterous Teleoperation

We first show the effectiveness of our vision-based teleoperation pipeline by examining how well the Snap Hand can copy the operator’s hand gesture. As shown in fig. 6, the Snap Hand can copy the operator’s hand accurately, accurately reproducing human grasping techniques, including

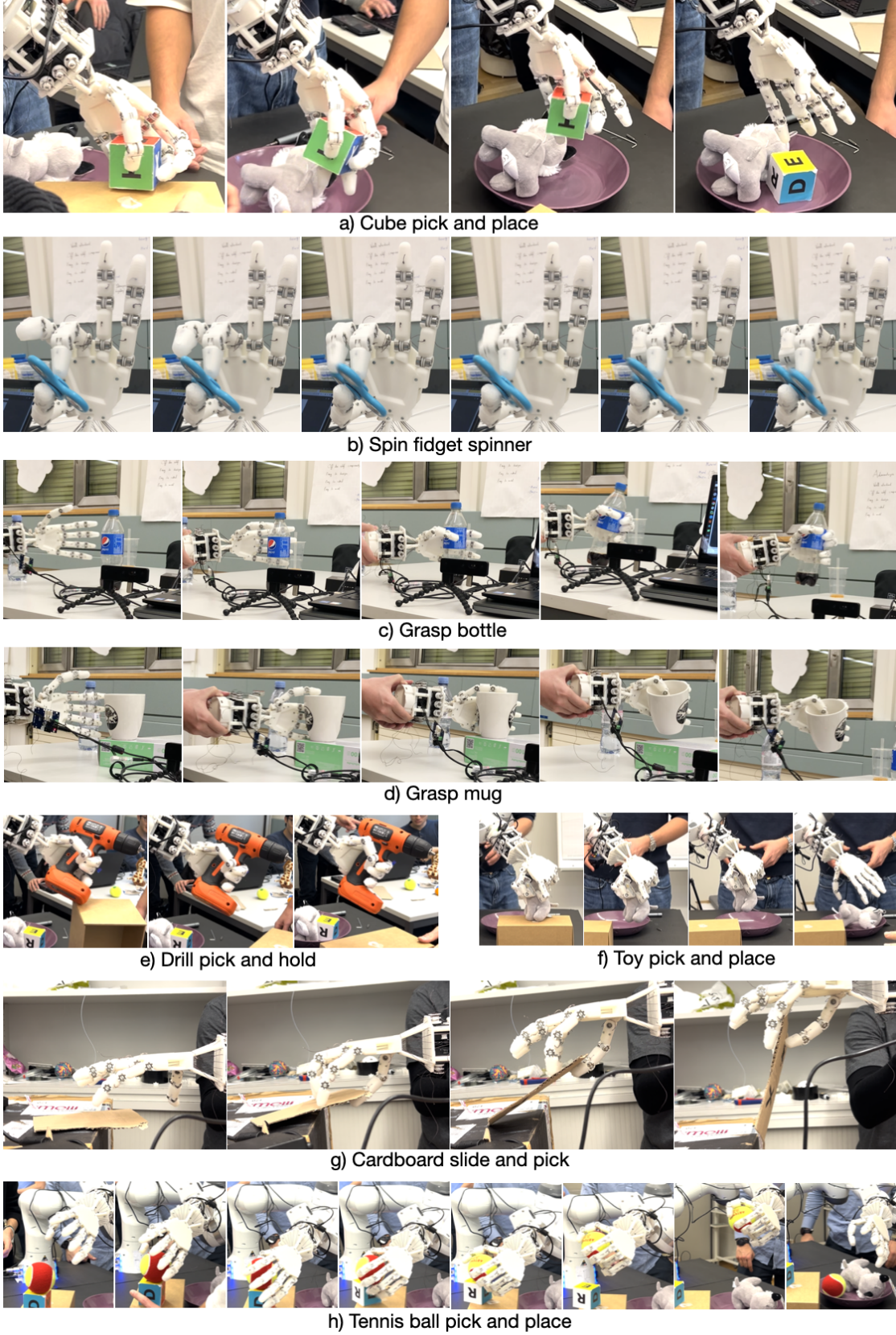


**Fig. 7: The Snap Hand performing various manipulation tasks through teleoperation.** Except for spinning the fidget spinner which is teleoperated through GUI, all tasks are performed through vision based teleoperation. Note the hand performs the tasks in a human-like manner due to its biomimetic design, proving its general-purpose capability.

precisely curling individual fingers independently and being able to pinch fingers together. This does not only prove the effectiveness of the teleoperation pipeline, but also validates the Snap Hand's biomimetic hardware design.

We conducted extensive experiments on a wide range of teleoperated manipulation tasks, including spinning a fidget spinner, grasping a plastic bottle and a mug, sliding cardboard along a surface to pick it up, picking up and grasping a drill conventionally, and picking up and grasping a cube, tennis ball, and toy, to show the general capability of the proposed Snap Hand. The snapshots of Snap Hands succeeding all the aforementioned tasks are presented in fig. 7. Due to the biomimetic form of the Snap Hand, it can accomplish all the above tasks in a human like manner, showing its general-purpose characteristics. All of the listed tasks are performed through vision-based teleroperation, except for spinning the fidget spinner, where the task is achieved through controlling the joints one by one through a GUI on the laptop. It is worth mentioning that although, we succeeded this task through vision based teleoperation as well, unfortunately no videos are recorded.

When attempting to operate a drill, the Snap Hand can successfully pick up the drill and hold it firmly. However, the finger is not strong enough to press the button to operate the drill continuously. We suspect that this is due to insufficient motor torque. A different finger shape, joint distribution, tendon layout, or range of motion with more motors could potentially solve the issue. It is also worth noting that the motors were not operating at their maximum torque, due to the desire to minimize the wear on the hand during the testing phase.

### B. RL-based Object Manipulation

In simulation, the Snap Hand is able to achieve a desired ball angular velocity of 0.1 rad/s, in the +x and -x axes as shown in fig. 8. It can also rotate the ball in the +y axis, albeit with a less robust policy. The successful policy is then simulated in an open loop, and successfully implemented onto the physical hand, with a slower command frequency. The hand is able to visibly rotate a ball (see fig. 9) although slippage results in a lower rotational velocity. This could also be due to discrepancies between the simulated ball radius and the real world ball, meaning that in the open loop policy the ball does not behave as the Snap Hand expects it to. Future work could focus on rectifying these problems with changes in the reinforcement learning policy as well as design changes to ensure adequate grip when in contact with the ball. Furthermore, either using sensors or computer vision, a closed loop policy could be implemented to try and limit the decrease in the ball's angular velocity when bridging the Sim2Real gap, allowing for real time reactions to the balls dynamics.

## VII. CONCLUSION

To conclude, the central problem addressed in this paper revolved around the design and conception of an affordable,

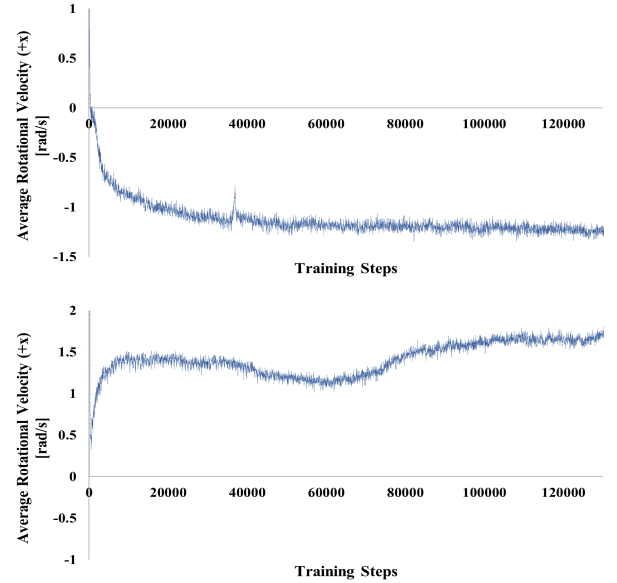


**Fig. 8: Average x-axis ball velocity [rad/s] vs. Reinforcement Learning Training Steps.** In simulation, the virtual Snap Hand learns to rotate the ball at angular velocities beyond the desired benchmark. The angular velocity begins to plateau at higher training steps as the agent now focuses on minimizing actuation effort and the rate at which the ball is dropped.

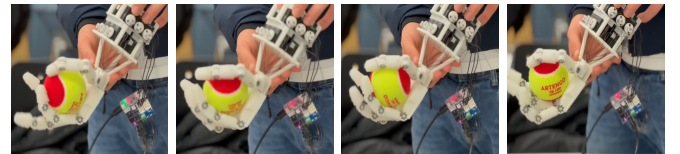


**Fig. 9: Sim2Real RL policy roll-out.** The Snap Hand open loop policy is able to keep the ball within the palm of the hand while opposing gravity with frequent periodic pushes along the top of the ball, resulting in rotation in the -x direction. The ball is also smaller than in the simulation, however the policy is still able to rotate it due to the ball radius being subject to random noise during the policy training process.

easily assembled robotic hand that could address the challenges faced by readily available grippers currently on the market. Mainly, the proposed solution aims to improve three aspects:

- Versatility by enabling interactions with a far wider range of objects;
- Ease of assembly by introducing the *snap joint*; and
- Trimming the design to a slim, elegant bio-mimetic solution capable of meeting the demands of modern human-robot interaction scenarios.

The novel joint design could pave the way to many exciting new opportunities. Future work could involve a way to take advantage of the quick assembly of the snap finger design to introduce interchangeable modular fingers. Each

would have a unique shape or set of sensors specifically designed for optimal compatibility with the task at hand. Switching to fingers with specific touch or heat sensors could have great benefits in terms of precision and safety within the work place. With some improvements to the tendon routing system currently in place, each finger could be interchanged in mere seconds. Having the robot learn to autonomously switch finger tips could also prove an exciting new iteration in the project.

## ACKNOWLEDGMENT

We would like to thank Prof. Robert Katzschmann, Alexander Kübler, and the entire RWR team for organizing the first edition of the Real World Robotics. We thank Andrea Nappi for designing the cool shirts and assisting with the experiments, Sebastiano Oliani for printing out all the 3d prints, Yifan Zhou for capturing the pictures and videos during the experiments, Benedek Forrai, Yasunori Toshimitsu, Gavin Cangan, Elvis Nava, Manuel Knecht, Stephan-Daniel Gravert, Thomas Buchner for the insightful talks, and Prof. Dogar Mehmet for the inspiring talk and discussions.

## REFERENCES

- [1] Z. Fu, T. Z. Zhao, and C. Finn, "Mobile aloha: Learning bimanual mobile manipulation with low-cost whole-body teleoperation," *arXiv preprint arXiv:2401.02117*, 2024.
- [2] Y. Toshimitsu, B. Forrai, B. G. Cangan, U. Steger, M. Knecht, S. Weirich, and R. K. Katzschmann, "Getting the ball rolling: Learning a dexterous policy for a biomimetic tendon-driven hand with rolling contact joints," in *2023 IEEE-RAS 22nd International Conference on Humanoid Robots (Humanoids)*, 2023, pp. 1–7.
- [3] OpenAI, I. Akkaya, M. Andrychowicz, M. Chociej, M. Litwin, B. McGrew, A. Petron, A. Paino, M. Plappert, G. Powell, R. Ribas, J. Schneider, N. Tezak, J. Tworek, P. Welinder, L. Weng, Q. Yuan, W. Zaremba, and L. Zhang, "Solving rubik's cube with a robot hand," *CoRR*, vol. abs/1910.07113, 2019. [Online]. Available: <http://arxiv.org/abs/1910.07113>
- [4] U. Kim, D. Jung, H. Jeong, J. Park, H.-M. Jung, J. Cheong, H. R. Choi, H. Do, and C. Park, "Integrated linkage-driven dexterous anthropomorphic robotic hand," *Nature communications*, vol. 12, no. 1, p. 7177, 2021.
- [5] Z. Ding, Y. Chen, A. Z. Ren, S. S. Gu, Q. Wang, H. Dong, and C. Jin, "Learning a universal human prior for dexterous manipulation from human preference," 2023.
- [6] Y. Qin, Y.-H. Wu, S. Liu, H. Jiang, R. Yang, Y. Fu, and X. Wang, "Dexmv: Imitation learning for dexterous manipulation from human videos," 2022.
- [7] E. Bauer, E. Nava, and R. K. Katzschmann, "Hifaive: Learning human-inspired dexterous manipulation with the faive robotic hand," in *Proceedings of the IPPC-IROS'23*, 2023. [Online]. Available: <https://ippc-iros23.github.io/papers/bauer.pdf>
- [8] S. R. Company, "Shadow dexterous hand series - research and development tool," 2023. [Online]. Available: <https://www.shadowrobot.com/dexterous-hand-series/>
- [9] W. Robotics, "Allegro hand: Highly adaptive robotic hand for r&d," 2023. [Online]. Available: <https://www.wonikrobotics.com/research-robot-hand>
- [10] K. Shaw, A. Agarwal, and D. Pathak, "Leap hand: Low-cost, efficient, and anthropomorphic hand for robot learning," 2023.
- [11] V. Makoviychuk, L. Wawrzyniak, Y. Guo, M. Lu, K. Storey, M. Macklin, D. Hoeller, N. Rudin, A. Allshire, A. Handa, and G. State, "Isaac gym: High performance gpu-based physics simulation for robot learning," 2021.
- [12] H. Liu, K. Wu, P. Meusel, N. Seitz, G. Hirzinger, M. Jin, Y. Liu, S. Fan, T. Lan, and Z. Chen, "Multisensory five-finger dexterous hand: The dlr/hit hand ii," in *2008 IEEE/RSJ International Conference on Intelligent Robots and Systems*, 2008, pp. 3692–3697.
- [13] D.-H. Lee, J.-H. Park, S.-W. Park, M.-H. Baeg, and J.-H. Bae, "Kitech-hand: A highly dexterous and modularized robotic hand," *IEEE/ASME Transactions on Mechatronics*, vol. 22, no. 2, pp. 876–887, 2017.
- [14] S. Shirafuji, S. Ikemoto, and K. Hosoda, "Development of a tendon-driven robotic finger for an anthropomorphic robotic hand," *Int. J. Rob. Res.*, vol. 33, no. 5, p. 677–693, apr 2014. [Online]. Available: <https://doi.org/10.1177/0278364913518357>
- [15] M. Grebenstein, M. Chalon, W. Friedl, et al., "The hand of the dlr hand arm system: Designed for interaction," *The International Journal of Robotics Research*, vol. 31, no. 13, pp. 1531–1555, 2012.
- [16] T. J. K. Buchner, S. Rogler, S. Weirich, Y. Armati, B. G. Cangan, J. Ramos, S. T. Twiddy, D. M. Marini, A. Weber, D. Chen, G. Ellison, J. Jacob, W. Zengerle, D. Katalichenko, C. Keny, W. Matusik, and R. K. Katzschmann, "Vision-controlled jetting for composite systems and robots," *Nature*, vol. 623, no. 7987, pp. 522–530, Nov 2023. [Online]. Available: <https://doi.org/10.1038/s41586-023-06684-3>
- [17] M. Tavakoli, R. Batista, and L. Sgrigna, "The uc softhand: Light weight adaptive bionic hand with a compact twisted string actuation system," *Actuators*, vol. 5, no. 1, 2016. [Online]. Available: <https://www.mdpi.com/2076-0825/5/1/1>
- [18] Y.-J. Kim, J. Yoon, and Y.-W. Sim, "Fluid lubricated dexterous finger mechanism for human-like impact absorbing capability," *IEEE Robotics and Automation Letters*, vol. 4, no. 4, pp. 3971–3978, 2019.
- [19] B. Dorner, "Chasing the colour glove: Visual hand tracking," Ph.D. dissertation, Simon Fraser University, 1994.
- [20] C. Theobalt, I. Albrecht, J. Haber, M. Magnor, H.-P. Seidel, and J. Marks, "Pitching a baseball - tracking high-speed motion with multi-exposure images," *ACM Transactions on Graphics*, v.23, 3, 540-547 (2004), vol. 23, 08 2004.
- [21] "Cyberglove systems," <http://www.cyberglovesystems.com>, accessed: 2024-01-11.
- [22] "Haptix," <https://haptix.com>, accessed: 2024-01-11.
- [23] "Manus," <https://www.manus-meta.com>, accessed: 2024-01-11.
- [24] Y. Rong, T. Shiratori, and H. Joo, "Frankmocap: A monocular 3d whole-body pose estimation system via regression and integration," in *IEEE International Conference on Computer Vision Workshops*, 2021.
- [25] A. Handa, K. Van Wyk, W. Yang, J. Liang, Y.-W. Chao, Q. Wan, S. Birchfield, N. Ratliff, and D. Fox, "Dexpilot: Vision-based tele-operation of dexterous robotic hand-arm system," in *2020 IEEE International Conference on Robotics and Automation (ICRA)*, 2020, pp. 9164–9170.
- [26] Google, "Mediapipe," <https://github.com/google/mediapipe>, accessed: 2024-01-11.
- [27] P. Weiner, J. Starke, F. Hundhausen, J. Beil, and T. Asfour, "The kit prosthetic hand: Design and control," in *2018 IEEE/RSJ International Conference on Intelligent Robots and Systems (IROS)*, 2018, pp. 3328–3334.
- [28] S. Shirafuji, S. Ikemoto, and K. Hosoda, "Development of a tendon-driven robotic finger for an anthropomorphic robotic hand," *The International Journal of Robotics Research*, vol. 33, no. 5, pp. 677–693, 2014.
- [29] L. B. Bridgwater, C. A. Ihrke, M. A. Diftler, M. E. Abdallah, N. A. Radford, J. M. Rogers, S. Yayathi, R. S. Askew, and D. M. Linn, "The robonaut 2 hand - designed to do work with tools," in *2012 IEEE International Conference on Robotics and Automation*, 2012, pp. 3425–3430.
- [30] The Robot Studio, "The human approach to robots," <https://www.therobotstudio.com/>, 2024, accessed: 2024-01-11.
- [31] D. Oh, Z. Li, J. Kim, H. Choi, H. Moon, and J. Koo, "A flexible self-recovery finger joint for a tendon-driven robot hand," *Review of Scientific Instruments*, vol. 91, no. 11, p. 115002, Nov 2020.